Coagulation by Random Velocity Fields as a Kramers Problem

Bernhard Mehlig[1] and Michael Wilkinson[2]

[1]*Physics and Engineering Physics, Gothenburg University/Chalmers, Gothenburg, Sweden*

[2]*Faculty of Mathematics and Computing, The Open University, Walton Hall, Milton Keynes, MK7 6AA, England*

(Received 22 October 2003; published 24 June 2004)

We analyze the motion of a system of particles suspended in a fluid which has a random velocity field. There are coagulating and noncoagulating phases. We show that the phase transition is related to a Kramers problem, and we use this to determine the phase diagram in two dimensions, as a function of the dimensionless inertia of the particles, ϵ, and a measure of the relative intensities of potential and solenoidal components of the velocity field, Γ. We find that the phase line is described by a function which is nonanalytic at $\epsilon = 0$, and which is related to escape over a barrier in the Kramers problem. We discuss the physical realizations of this phase transition.

DOI: 10.1103/PhysRevLett.92.250602 PACS numbers: 05.10.Gg, 05.40.–a, 46.65.+g

Deutsch [1] introduced and investigated a model which can describe the motion of particles suspended in a randomly moving fluid. He showed that the one-dimensional model exhibits a phase transition between coagulating and noncoagulating phases as the effect of inertia of the particles is increased. We recently solved Deutsch's one-dimensional model exactly ("path-coalescence model" [2]).

This Letter discusses the phase diagram for the path-coalescence model in higher dimensions, the most relevant case for physical applications, involving the dynamics of inertial particles suspended in a randomly moving gas. This problem has attracted considerable interest in the context of, for example, tracer particles in turbulent flow [3,4], cloud formation [5], and aggregation of interstellar dust [6], the aggregation of buoyant particles on the surface of a turbulent liquid [7]. It is also relevant to ultrasonic aggregation of aerosols [8] as we shall show.

In the limit where inertial effects are negligible, the suspended particles are advected by the flow: The theory of this limiting case is described in [9]. However, the case where the inertia of the particles plays an important role is much less thoroughly understood. In Ref. [3], a model is described in which inertial effects are treated by assuming that particles are advected in a perturbed velocity field. Reference [4] gives numerical results on particle aggregation in a closely related model. Here we give a treatment of the phase transition in two dimensions (Fig. 1), using an exact mapping to a Kramers problem (the escape of particles from an attractor by diffusion).

We derive a perturbation expansion for a Lyapunov exponent λ_1 determining the phase transition, in powers of a dimensionless measure of the inertia, ϵ. We show that there is a nonanalytical contribution $\delta\lambda_1$ to the perturbation series for λ_1. This nonanalytic term is characteristic of the flux over a barrier in a Kramers problem: $\delta\lambda_1 \sim \exp(-\Phi/\epsilon^2)$, where Φ is the action of a trajectory in a Hamiltonian dynamical system. We conclude with a discussion of ultrasonic aggregation.

We consider noninteracting spherical particles of mass m, radius a, and $\boldsymbol{r}(t)$ denotes the position of a typical particle. These move through a fluid with velocity $\boldsymbol{u}(\boldsymbol{r}, t)$ having viscosity η. To avoid complications from displaced-mass effects [10], we assume that the particles have much higher density than the surrounding fluid. Our results are therefore most relevant to suspensions in gases, and we allow $\boldsymbol{u}(\boldsymbol{r}, t)$ to be a compressible flow (by contrast, Refs. [3,4] treat the case relevant to suspensions in liquids). We consider the case where the drag force $\boldsymbol{f}_{\rm dr}$ on the particle is given by Stokes's law: $\boldsymbol{f}_{\rm dr} = 6\pi\eta a(\boldsymbol{u} - \dot{\boldsymbol{r}})$. The equation of motion is

$$\ddot{\boldsymbol{r}} = -\gamma(\dot{\boldsymbol{r}} - \boldsymbol{u}), \tag{1}$$

where $\gamma = 6\pi\eta a/m$. Rearranging (1) gives $\dot{\boldsymbol{r}} = \boldsymbol{p}/m$, $\dot{\boldsymbol{p}} = -\gamma\boldsymbol{p} + \boldsymbol{f}(\dot{\boldsymbol{r}}, t)$, where $\boldsymbol{f} = \gamma m\boldsymbol{u}$ will be modeled by a random field. Linearizing to obtain an equation for the separation $(\delta\boldsymbol{r}, \delta\boldsymbol{p})$ of two nearby trajectories gives

$$\delta\dot{\boldsymbol{r}} = \delta\boldsymbol{p}/m, \qquad \delta\dot{\boldsymbol{p}} = -\gamma\delta\boldsymbol{p} + \mathbf{F}(t)\delta\boldsymbol{r}, \tag{2}$$

where $\mathbf{F}(t)$ is a 2×2 matrix with elements $F_{ij}(t) = \partial f_i/\partial r_j(\mathbf{r}(t), t)$. We write $\delta\boldsymbol{r} = X\hat{\boldsymbol{n}}_\theta$ and $\delta\boldsymbol{p} = Y_1 X\hat{\boldsymbol{n}}_\theta +$

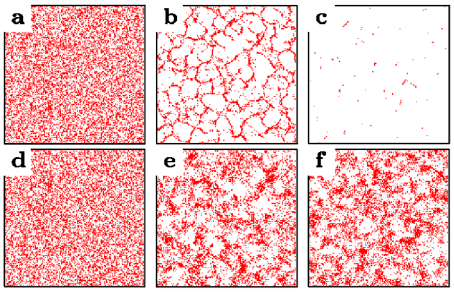

FIG. 1 (color online). Evolution of uniform initial particle distribution under Eq. (1) in the unit square with periodic boundary conditions, for 10^4 particles; $\Gamma = 1/3$, $\epsilon = 0.33$ (coalescing phase), at $t = 0$ (a), 10 (b), and $t = 275$ (c); $\Gamma = 1/3$, $\epsilon = 4.30$ at $t = 0$ (d), 10 (e), and 275 (f). The statistics of the force is explained in the text; we chose $C(R, \Delta t) \propto \exp[-\Delta t^2/(2\tau^2) - R^2/(2\xi^2)]$ with $\xi = 0.1/\pi$ and $\tau \to 0$.

$Y_2 X \hat{\boldsymbol{n}}_{\theta+\pi/2}$, where $\hat{\boldsymbol{n}}_\theta$ is unit vector in direction θ. We expect that the scale variable X may increase or decrease, but that θ, Y_1, and Y_2 approach a stationary distribution.

The phase transition is determined by the behavior of X: If the (maximal) Lyapunov exponent $\lambda_1 = m^{-1} d\langle \log_e X\rangle/dt$ is negative, the particles coagulate [2]. Substituting the expressions for $\delta \boldsymbol{r}$ and $\delta \boldsymbol{p}$ into (2), and taking scalar products with $\hat{\boldsymbol{n}}_\theta$ and $\hat{\boldsymbol{n}}_{\theta+\pi/2}$, we obtain

$$\dot{X} = Y_1 X/m, \qquad \dot{\theta} = Y_2/m, \tag{3}$$

and

$$\begin{aligned} \dot{Y}_1 &= (Y_2^2 - Y_1^2)/m - \gamma Y_1 + F_{\mathrm{d}}(t), \\ \dot{Y}_2 &= -2Y_1 Y_2/m - \gamma Y_2 + F_{\mathrm{o}}(t), \end{aligned} \tag{4}$$

where $F_{\mathrm{d}}(t) = \hat{\boldsymbol{n}}_\theta \cdot \mathbf{F}(t) \hat{\boldsymbol{n}}_\theta$ and $F_{\mathrm{o}}(t) = \hat{\boldsymbol{n}}_{\theta+\pi/2} \cdot \mathbf{F}(t) \hat{\boldsymbol{n}}_\theta$. From (3), the distribution of θ becomes uniform on $[0, 2\pi]$ at large t, and the Lyapunov exponent is

$$\lambda_1 = \langle Y_1 \rangle / m. \tag{5}$$

The statistics of the random force is assumed to be rotationally invariant, so that the statistics of F_{d} and F_{o} are independent of θ. For $\theta = 0$, we have $F_{\mathrm{d}} = F_{11}$ and $F_{\mathrm{o}} = F_{21}$, so we obtain the statistics of F_{d}, F_{o} from those of F_{11}, F_{21}. Equations (4) are thus independent of (3). The Lyapunov exponent is therefore determined by solving a pair of coupled stochastic differential equations for (Y_1, Y_2).

To make further progress, we must specify the statistical properties of the isotropic and homogeneous random field $\boldsymbol{f}$. We consider the case where $\langle \boldsymbol{f} \rangle = 0$. Without loss of generality, we can write

$$\boldsymbol{f}(\boldsymbol{r}, t) = \nabla \phi(\boldsymbol{r}, t) + \nabla \wedge \hat{\boldsymbol{n}}_3 \psi(\boldsymbol{r}, t), \tag{6}$$

where $\hat{\boldsymbol{n}}_3$ is a unit vector pointing out of the plane. The components of $\boldsymbol{f}$ arising from ϕ and ψ are termed the potential and solenoidal components, respectively. In the following, we assume that the correlation function $C(R, \Delta t) = \langle \phi(\boldsymbol{r}, t) \phi(\boldsymbol{r}', t') \rangle$ is an even function of $\Delta t = t - t'$ with support τ (the correlation time), and has support ξ (the correlation length) in $R = |\boldsymbol{r} - \boldsymbol{r}'|$. We also assume, for simplicity, that the fields ϕ and ψ are not correlated with each other, and have the same correlation functions, apart from a scale factor $\alpha^2 = \langle \psi^2 \rangle / \langle \phi^2 \rangle$. These assumptions are easily relaxed.

If the correlation time τ is short compared to other relevant time scales, we can write (4) as a pair of coupled Langevin equations. We scale these into a dimensionless form, in which the diffusion matrix is the unit matrix

$$\begin{aligned} dx_1 &= [-x_1 + \epsilon(\Gamma x_2^2 - x_1^2)] dt' + dw_1, \\ dx_2 &= [-x_2 - 2\epsilon x_1 x_2] dt' + dw_2. \end{aligned} \tag{7}$$

Here $x_i = \sqrt{\gamma/D_i}\, Y_i$ (for $i = 1, 2$), $t' = \gamma t$, $\langle dw_i \rangle = 0$, $\langle dw_i dw_j \rangle = 2\delta_{ij} dt'$, and

$$D_i = \frac{1}{2} \int_{-\infty}^{\infty} dt \langle F_{i1}(t) F_{i1}(0) \rangle. \tag{8}$$

The two parameters Γ and ϵ are defined as follows:

$$\Gamma \equiv D_2/D_1 = (1 + 3\alpha^2)/(3 + \alpha^2) \tag{9}$$

characterizes the ratio of the solenoidal and potential field amplitudes, $\frac{1}{3} \le \Gamma \le 3$, with $\Gamma = \frac{1}{3}$ for purely potential fields, $\Gamma = 3$ for pure solenoidal force fields, and $\Gamma = 1$ for equal field intensities. The second parameter,

$$\epsilon = D_1^{1/2}/(m\gamma^{3/2}) = (mD_1)^{1/2}/(6\pi\eta a)^{3/2}, \tag{10}$$

is a measure of the importance of inertial effects in the equation of motion.

The Langevin equations (7) are equivalent to a Fokker-Planck equation [11]:

$$\frac{\partial P}{\partial t'} = \hat{\mathcal{F}} P \equiv \nabla \cdot [-\boldsymbol{V} P + \nabla P], \tag{11}$$

where the advection field $\boldsymbol{V}$ has components $V_1 = -x_1 + \epsilon(\Gamma x_2^2 - x_1^2)$ and $V_2 = -x_2 - 2\epsilon x_1 x_2$. We write $\hat{\mathcal{F}} = \hat{\mathcal{F}}_0 + \epsilon \hat{\mathcal{F}}_1$ and seek a steady-state solution P satisfying $\hat{\mathcal{F}} P = 0$. The Lyapunov exponent λ_1 is determined by computing $\langle x_1 \rangle$ with $P(\boldsymbol{x})$, and using (5) to obtain $\lambda_1 = \gamma\epsilon\langle x_1 \rangle$.

We start by considering a perturbative approach. In the limit $\epsilon \to 0$, the steady-state solution is

$$P_0(\boldsymbol{x}) = A \exp\left[-\frac{1}{2}(x_1^2 + x_2^2) \right] \equiv A \exp[-\Phi_0(\boldsymbol{x})]. \tag{12}$$

It is convenient to make a transformation of the Fokker-Planck operator $\hat{\mathcal{F}}$ to a new operator $\hat{\mathcal{H}}$ of the form [11] $\hat{\mathcal{H}} = \exp(\Phi_0/2) \hat{\mathcal{F}} \exp(-\Phi_0/2)$. We write $\hat{\mathcal{H}} = \hat{\mathcal{H}}_0 + \epsilon \hat{\mathcal{H}}_1$ and obtain, for $\hat{\mathcal{H}}_0$,

$$\hat{\mathcal{H}}_0 = \left(\partial_{x_1}^2 - \frac{1}{4} x_1^2 \right) + \left(\partial_{x_2}^2 - \frac{1}{4} x_2^2 \right) + 1, \tag{13}$$

where $(\partial_{x_i}^2 - x_i^2/4)$ are one-dimensional quantum-mechanical harmonic-oscillator Hamiltonians for coordinates x_i. The eigenvalues of $\hat{\mathcal{H}}_0$ are $-(k + l)$, where k and l are non-negative integers. We use a variant of Dirac notation denoting the eigenstates of $\hat{\mathcal{H}}_0$ by $|\phi_{kl}\rangle$, with $(\boldsymbol{x}|\phi_{00}) = \exp[-\Phi_0(\boldsymbol{x})/2]$, and $P(\boldsymbol{x}) = (\boldsymbol{x}|P)$. Introducing annihilation and creation operators, $\hat{a}_i$ and $\hat{a}_i^\dagger$, with the usual properties, such that $\hat{x}_i = \hat{a}_i + \hat{a}_i^\dagger$, we find

$$\hat{\mathcal{H}}_1 = \hat{a}_1^\dagger (\Gamma \hat{x}_2^2 - \hat{x}_1^2) - 2\, \hat{a}_2^\dagger \hat{x}_2 \hat{x}_1. \tag{14}$$

We seek a null eigenvector of $\hat{\mathcal{H}}$, satisfying $\hat{\mathcal{H}}|Q) = 0$, in the form of a perturbation series, $|Q) = |Q_0) + \epsilon|Q_1) + \epsilon^2 |Q_2) + \cdots$, where $|Q_0) = |\phi_{00})$. The general term satisfies the recursion $\hat{\mathcal{H}}_0 |Q_{n+1}) + \hat{\mathcal{H}}_1 |Q_n) = 0$. In terms of $|Q)$, the expectation of x_1 is given by

$$\langle x_1 \rangle = (\phi_{00}|\hat{a}_1|Q)/(\phi_{00}|Q). \tag{15}$$

We find that $(\phi_{00}|Q) = 1$ in all orders of perturbation theory. Evaluating $(\phi_{00}|\hat{a}_1|Q)$, we find that all of the even orders vanish, and that in the odd orders the square roots arising from the action of annihilation and creation

operators cancel, so that the perturbation series for $\langle x_1 \rangle$ has integer coefficients. We obtain

$$\lambda_1 = -\gamma \sum_{k \geq 1} c_k [(1-\Gamma)\epsilon^2]^k, \tag{16}$$

with $c_1 = 1$, $c_2 = 5$, $c_3 = 60$, $c_4 = 1105$, $c_5 = 27\,120$, $c_6 = 828\,250, \ldots$. This predicts that the Lyapunov exponent is positive (noncoagulating phase) for $\Gamma > 1$ and negative for $\Gamma < 1$, independent of ϵ. Figure 2(b) shows that this surprising prediction is indeed false.

It is possible that the Lyapunov exponent may have a component nonanalytic at $\epsilon = 0$, not captured by perturbation theory. The series (16) is asymptotic and should be truncated at the smallest term, with index k^*. The coefficients satisfy the recursion $c_k = (6k-8)c_{k-1} + \sum_{l=1}^{k-1} c_l c_{k-l}$ with $c_0 = -1/2$, and we find

$$c_k \sim 3^k \sqrt{2k!} \tag{17}$$

for $k \to \infty$, so that $k^* \sim 1 + \mathrm{Int}\{1/[6(1-\Gamma)\epsilon^2]\}$, where $\mathrm{Int}\{x\}$ is the integer part of x. We apply a principle expounded by Dingle [12], which suggests that the error of an asymptotic series is comparable to its smallest term. This approach indicates that in the limit $\epsilon \to 0$ the nonanalytic term is of the form $\delta\lambda_1 \sim C \exp\{-1/[6(1-\Gamma)\epsilon^2]\}$ (where C might have a power-law dependence on ϵ). This still incorrectly predicts that the nonanalytic contribution vanishes at $\Gamma = 1$ (i.e., that the phase line is independent of ϵ).

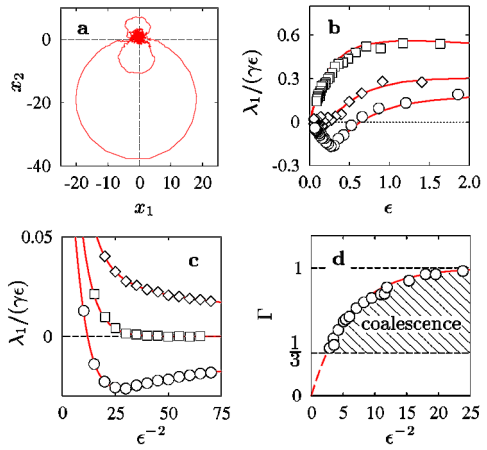

FIG. 2 (color online). (a) A trajectory for the Langevin equations, (7), for $\epsilon = 0.5$, $\Gamma = 1$, and $0 \leq t' \leq 10^2$. The trajectory $\boldsymbol{x}(t)$ is most frequently located close to the origin, but occasionally it passes the unstable fixed point at $(-1/\epsilon, 0)$, making a large excursion before returning to the origin. The nonanalytic contribution to the Lyapunov exponent is associated with these large excursions. (b) Lyapunov exponent as a function of ϵ, for $\Gamma = \frac{1}{3}$ (○), 1 (◇), 3 (□): Monte Carlo simulations of (7) (lines) and integration of (1) (symbols). (c) Comparison of Monte Carlo simulation of (7) (symbols) and Eq. (19) (lines), for $\Gamma = 0.85$ (○), 1 (□), 1.15 (◇) (with $\chi = 0.34, 0.28, 0.215$). (d) Phase diagram in two dimensions: Monte Carlo simulations (○) of (7); the solid line is the function $1 - \Gamma = \exp[-1/(6\epsilon^2)]$.

We have therefore used an alternative approach to extract the nonanalytic term missing in the optimally truncated perturbation series: We write P as $P = A \exp[-\Phi(\boldsymbol{x})]$ so that Φ must satisfy

$$\nabla^2\Phi - \nabla \cdot \boldsymbol{V} - \boldsymbol{V} \cdot \nabla\Phi - (\nabla\Phi)^2 = 0. \tag{18}$$

The deterministic advection velocity field $\boldsymbol{V}$ contains terms which are quadratic in $\boldsymbol{x}$. This suggests that Φ is bounded by a cubic in $\boldsymbol{x}$. In (18), the first two terms are expected to be bounded by multiples of $|\boldsymbol{x}|$, whereas the remaining terms are expected to be bounded by a cubic function of $|\boldsymbol{x}|$. We expect that, close to the origin, the solution is well approximated by $\Phi \sim \Phi_0 = \frac{1}{2}(x_1^2 + x_2^2)$, and that far from the origin Φ is well approximated by the solution of the equation containing only the leading-order terms, i.e., $\boldsymbol{V} \cdot \nabla\Phi + (\nabla\Phi)^2 = 0$. This has the form of a Hamilton-Jacobi equation $H(\boldsymbol{x}, \nabla\Phi) = E$, where in our case $E = 0$ and where the Hamiltonian is [13] $H(\boldsymbol{x}, \boldsymbol{p}) = \boldsymbol{V}(\boldsymbol{x}) \cdot \boldsymbol{p} + \boldsymbol{p}^2$. The Hamilton-Jacobi equation is solved by integrating Hamilton's equations, then Φ is obtained by integration along the trajectories: $\Phi(\boldsymbol{x}) = \int^t dt' \, \dot{\boldsymbol{x}} \cdot \boldsymbol{p}$. We start classical trajectories infinitesimally close to the origin with initial conditions $\boldsymbol{p} = \nabla\Phi = \boldsymbol{x}$, integrate them numerically, investigate the form of the trajectories, and determine the action function $\Phi(\boldsymbol{x})$. We are especially interested in singularities of Φ, because these are expected to lead to nonanalytic behavior of the Lyapunov exponent.

On the x_1 axis, for $p_2 = 0$, the vectors $\dot{\boldsymbol{x}}$, $\boldsymbol{V}$, and $\boldsymbol{x}$ are parallel, and $\boldsymbol{p} = -\boldsymbol{V}$. This trajectory crosses a singularity at the point $\boldsymbol{x}^* = (-1/\epsilon, 0)$, at which both $\boldsymbol{V}$ and $\boldsymbol{p}$ vanish, with action $\Phi(-1/\epsilon, 0) = 1/(6\epsilon^2)$. For $0 < \Gamma < 2$, our numerical experiments did not identify any other singular point with a smaller value of Φ. Consider the physical significance of this singular point in terms of the dynamics of a fictitious particle with position $\boldsymbol{x}(t)$ described by the Langevin Eq. (7). A typical trajectory is plotted in Fig. 2(a). The advection field $\boldsymbol{V}$ has an unstable fixed point at $\boldsymbol{x}^*$. To the right of the singularity, the particle is advected back towards the origin, and the probability density decreases rapidly as the fixed point is approached from that direction. To the left of the singularity, the particle is advected away, following the advection field $\boldsymbol{V}$: Initially it moves to the left, returning to large positive x_1 in a large circuit. The singularity is therefore associated with diffusive escape from the attractor of $\boldsymbol{V}$ at $\boldsymbol{x} = 0$, in which the escaping particle is initially advected away, but returns along paths close to the positive x_1 axis. This leads to the hypothesis that there should be a contribution to λ_1 proportional to $\exp[-\Phi(\boldsymbol{x}^*)] = \exp[-1/(6\epsilon^2)]$, where the prefactor may have an algebraic dependence on ϵ.

According to our numerical results, the dominant correction to the perturbation series in the limit $\epsilon \to 0$ does indeed arise in this way: We find

$$\lambda_1/\gamma \sim \chi(\Gamma)\exp[-1/(6\epsilon^2)] - \sum_{k=1}^{k^*} c_k[(1-\Gamma)\epsilon^2]^k. \quad (19)$$

We have not been able to determine the form of the prefactor χ analytically: It appears to be independent of ϵ. In Fig. 2(c), we compare the Monte Carlo simulations of (7) with (19). Figure 2(d) shows the phase diagram, as determined using (5) and Monte Carlo simulation of (7). The computed curve is compared with an empirical fit, using the exponential function $\exp[-1/(6\epsilon^2)]$ which characterizes the escape process.

The coefficients in (16) also occur in the asymptotic expansion of $\mathrm{Ai}'(z)/\mathrm{Ai}(z)$ [14]. This suggests that $\lambda_1/\gamma = -\mathrm{Re}\,[\mathrm{Ai}'(z)/\mathrm{Ai}(z) + \sqrt{z}]/(2\sqrt{z})$ with $z = (i\sqrt{1-\Gamma}\epsilon)^{-4/3}/4$. This expression cannot be correct for $|1-\Gamma| < 1$, because its leading-order nonanalytic correction becomes smaller than the nonanalytic term in (19) in the limit $\epsilon \to 0$. However, on setting $\Gamma = 0$, we find that it does agree with the exact solution of the one-dimensional problem obtained in [2], and our numerical results show excellent agreement with Monte Carlo simulations when $\Gamma = 2$ (where we believe that it could also be exact), and when $\Gamma = 3$.

In summary, we have seen that the theory of coagulation by random velocity fields bears several surprises. We have seen that the phase transition is determined by the stationary state of a Langevin process. Perturbation theory incorrectly predicts that the phase line is independent of the inertia parameter ϵ. The asymptotics of the high order terms of the perturbation series again do not predict the correct form of the nonanalytic term; we are not aware of any other physical example where this procedure fails (although a mathematical example was suggested in [15]). Finally, the path-coalescence phase transition is driven by a nonanalytic term characterizing the flux of a barrier in a Kramers problem.

We conclude with a number of remarks and a discussion of possible applications of the effect. First, in many applications the suspended particles will not have equal masses, and it is necessary to consider how mass dispersion affects the coagulation process. We have shown, in a perturbative framework, that two particles with masses differing by $\delta m \ll m$ follow trajectories with separation $\Delta \boldsymbol{r} = \delta m \boldsymbol{g}(t)$, where $\langle|\boldsymbol{g}(t)|^2\rangle$ remains bounded as $t \to \infty$. We infer that, when the masses are unequal, particles condense onto fragmented line segments rather than isolated points. The coagulation effect is therefore weakened, but not destroyed (Fig. 3) by mass dispersion. Second, the structures observed in Fig. 1(b) indicate that the area-contraction rate is much larger than the maximal Lyapunov exponent λ_1. We have verified this by computing the Lyapunov spectrum $\lambda_4 < \lambda_3 < \lambda_2 < \lambda_1$ of (1) numerically (the area-contraction rate is given by $\lambda_2 + \lambda_1$).

Turning to specific applications, we note that the random velocity field $\boldsymbol{u}(\boldsymbol{r}, t)$ could arise from random sound waves, turbulent flow, or other random disturbances. We do not know how to estimate Γ reliably for turbulent flow in gases. In the case of liquids where the flow is incompressible, our theory applies when the suspended particles are denser that the fluid: We predict there is no coagulation because $\Gamma > 1$. In sound waves the velocity field is proportional to the pressure gradient, and is therefore pure potential: $\Gamma = \frac{1}{3}$, so according to Fig. 2(d) there is a coagulating phase. One possible technological application of the effect would be to the coagulation of small pollutant particles in an engine exhaust. An ultrasonic noise source could increase the size of the pollutant particles until they are large enough to be captured efficiently by a mechanical filter. Coagulation by ultrasonic sources has been observed experimentally [8]. Theoretical treatments, reviewed in [8], have considered the case where the ultrasound has a single frequency, and the coagulation results from particles with differing masses experiencing different displacements. This Letter has introduced a new mechanism for ultrasonic coagulation, which works even when particles have the same mass.

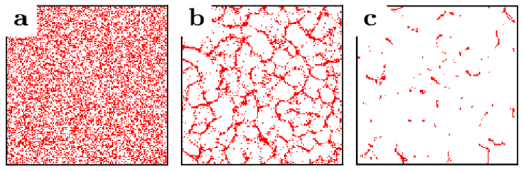

FIG. 3 (color online). Same as Fig. 1(a)–1(c), but with masses uniformly distributed on an interval of half width $\delta m = 0.2\langle m\rangle$.

[1] J. M. Deutsch, J. Phys. A **18**, 1457 (1985).
[2] M. Wilkinson and B. Mehlig, Phys. Rev. E (to be published).
[3] E. Balkovsky, G. Falkovitch, and A. Fouxon, Phys. Rev. Lett. **86**, 2790 (2001).
[4] J. Bec, nlin/0306049, 2003.
[5] R. A. Shaw, Annu. Rev. Fluid Mech. **35**, 183 (2003).
[6] A. Johansson *et al.*, astro-ph/0310059, 2003.
[7] Jörg Schumacher and B. Eckhardt, Phys. Rev. E **66**, 017303 (2002).
[8] G. L. Gooberman, *Ultrasonics: Theory and Application* (Hart Publications, New York, 1969).
[9] V. I. Klyatskin and D. Gurarie, Phys. Usp. **42**, 165 (1999).
[10] L. D. Landau and E. M. Lifshitz, *Fluid Mechanics* (Pergamon, Oxford, 1959).
[11] H. Risken, *The Fokker-Planck Equation. Methods of Solutions and Applications* (Springer, New York, 1999).
[12] R. B. Dingle, *Asymptotic Expansions: Their Derivation and Interpretation* (Academic, New York, 1974).
[13] M. I. Freidlin and A. D. Wentzell, *Random Perturbations of Dynamical Systems* (Springer, New York, 1984).
[14] M. Prähofer, in On-Line Encyclopaedia of Integer Sequences, A062980 (2001), available online at http://www.research.att.com/~njas/sequences
[15] R. Balian, G. Parisi, and A. Voros, in *Lecture Notes in Physics* (Springer, New York, 1979), Vol. 106.